A Multitrace Surface Integral Equation Method for PEC/Dielectric Composite Objects

Ran Zhao, *Member, IEEE*, Ping Li, *Senior Member, IEEE*, Jun Hu, *Senior Member, IEEE*, and Hakan Bagci, *Senior Member, IEEE*

***Abstract*—The multitrace domain decomposition surface integral equation (MT-DD-SIE) originally developed to analyze electromagnetic scattering from dielectric composite objects is extended to efficiently account for perfect electrically conducting (PEC) bodies. This is achieved by adopting Robin transmission conditions (RTCs) to PEC surfaces. These PEC-RTCs, which are the only governing equations for a PEC body, are used to "couple" it to the dielectric bodies. Upon discretization, PEC-RTCs produce a well-conditioned matrix block and, therefore, does not negatively affect the convergence of the iterative solution of the MT-DD-SIE matrix equation. The resulting method is significantly faster and has a smaller memory footprint than the traditional globally coupled contact-region-modeling method that uses the coupled electric field and Poggio–Miller–Chang–Harrington–Wu–Tsai SIEs in analyzing electromagnetic scattering from composite PEC/dielectric objects. This is demonstrated by numerical examples involving electrically large scatterers.**

***Index Terms*—Composite objects, domain decomposition, electromagnetic scattering, locally coupled, multitrace.**

I. Introduction

ELECTROMAGNETIC scattering from composite objects consisting of piecewise homogeneous dielectric and/or perfect electrically conducting (PEC) bodies can be analyzed by solving various types of surface integral equations (SIEs) [1], [2]. For example, one can couple the electric field and Poggio–Miller–Chang–Harrington–Wu–Tsai integral equations (EFIE-PMCHWT) [3]–[5]. However, discretizing this coupled system of first-kind integral equations using the Rao–Wilton–Glisson (RWG) [26] functions yields an ill-conditioned matrix equation whose solution calls for a large number of iterations, especially for electrically large scatterers [6]. The convergence rate of the iterative search of the solution can be increased if second-kind integral equations are used: The combined-field integral equation (CFIE) and the electric–magnetic field CFIE (JMCFIE) [7]–[9], [28] can replace EFIE and PMCHWT on PEC and dielectric surfaces, respectively. Note that the magnetic-field integral equation (MFIE) and the Müller formulation are used to construct CFIE and JMCFIE, respectively. The RWG-based discretization of MFIE loses accuracy in the scattering analysis of PEC surfaces with sharp edges or corners. This is less evident for the Müller formulation on dielectric surfaces. On the other hand, the Müller formulation is known to be less accurate than PMCHWT for high-contrast dielectrics [29], [30]. Furthermore, RWG-based discretizations of MFIE and Müller are not conforming, therefore one has to use more complicated mixed-discretization schemes to increase the accuracy [31]–[33].

The multitrace SIEs [10], the contact-region modeling method (CRM) [11], and the domain decomposition method (DDM) [12]–[18] avoid tedious junction basis functions by introducing two sets of SIEs and unknown equivalent currents on the same surface between any two (sub) domains. Upon discretization, multitrace formulations result in a larger matrix system but the easier meshing process and the improved matrix conditioning are often worth the increase in the matrix dimension. Note that the junction basis functions can also be avoided without requiring two sets of unknowns on the same surface through the use of a monopolar RWG-based discretization [19]. DDM utilizes CFIE or JMCFIE as the governing equation to ensure a well-conditioned matrix system [12]–[18]. CRM, which uses EFIE-PMCHWT, yields a more accurate solution, but its application to electrically large scatterers is limited because of the resulting ill-conditioned matrix system [11].

In [25], a multitrace domain decomposition surface integral equation (MT-DD-SIE) method has been developed for analyzing scattering from composite objects consisting of multiple dielectric bodies (subdomains) (no PEC bodies are included). This method uses EFIE and MFIE as the governing equations (in unknown equivalent currents) in each subdomain, and these currents on the subdomain surfaces are locally coupled via the Robin transmission conditions (RTCs) [14], [21], [22]. The RWG-based discretization of this locally coupled system yields a matrix system that does not suffer from any ill-conditioning. In addition, the well-conditioned matrix blocks pertinent to the subdomains are used to generate a preconditioner that further accelerates the iterative solution of the locally coupled final matrix equation [23], [27]. This method is as accurate as CRM, but its memory requirement is significantly less.

Manuscript received March 18, 2021; revised May 6, 2021 and May 18, 2021; accepted May 18, 2021. Date of publication May 25, 2021; date of current version August 4, 2021. This work was supported in part by the National Natural Science Foundation of China under Grant 62031010 and Grant 61801002 and in part by KAUST OSR under Award 2019-CRG8-4056. *(Corresponding author: Ping Li.)*

Ran Zhao is with Anhui University, Hefei 230000, China, and also with the Division of Computer, Electrical, and Mathematical Science and Engineering, King Abdullah University of Science and Technology, Thuwal 23955, Saudi Arabia (e-mail: ran.zhao@kaust.edu.sa).

Ping Li is with the Key Laboratory of Ministry of Education of China for Research of Design and Electromagnetic Compatibility of High Speed Electronic Systems, Shanghai Jiao Tong University, Shanghai 200240, China, and also with the Shenzhen Institute of Research and Innovation, The University of Hong Kong, Shenzhen 518172, China (e-mail: ping.li@sjtu.edu.cn).

Jun Hu is with the School of Electronic Science and Engineering, University of Electronic Science and Technology of China, Chengdu 611731, China (e-mail: hujun@uestc.edu.cn).

Hakan Bagci is with the Division of Computer, Electrical, and Mathematical Science and Engineering, King Abdullah University of Science and Technology, Thuwal 23955, Saudi Arabia (e-mail: hakan.bagci@kaust.edu.sa).

Digital Object Identifier 10.1109/LAWP.2021.3082536

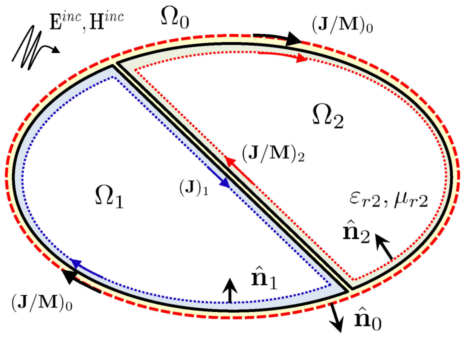

Fig. 1. Subdomains defined for a PEC/dielectric composite scatterer and the variables associated with them.

In [24], a multitrace method has been developed for composite objects consisting of dielectric bodies and a PEC surface. This method uses PMCHWT as the governing equation and the equivalent currents on the surfaces between the dielectric subdomains are coupled using RTCs. The currents on the PEC surface are accounted for in the governing equations of the subdomains that are "touching" to it. The condition number of the final matrix equation increases very quickly when the size of the PEC surface is electrically large prohibiting its iterative solution. In addition, when this method is applied to partially coated objects, it requires a special treatment of the discretization, which involves half-RWG functions, at the interface between the PEC and dielectric surfaces.

In this letter, these bottlenecks are eliminated by using a special form of RTCs as the only governing equations on the PEC bodies (subdomains) within MT-DD-SIE [25]. Consequently, the matrix blocks pertinent to the PEC subdomains, which are similar to the sparse Gram matrix obtained from the discretization of the self-term in CFIE, are well-conditioned. Therefore, the well-conditioning of the MT-DD-SIE matrix is maintained even after the PEC subdomains are accounted for. Note that PEC-RTCs have been first proposed in [20], but they are used to avoid the issues arising from strong coupling between subdomains introduced within a PEC cavity. In this letter, they are used to efficiently and accurately account for the PEC bodies within a multitrace SIE method developed for composite objects.

II. Formulation

A. *Multitrace Domain Decomposition Surface Integral Equation*

Let Ω represent the support of a PEC/dielectric composite scatterer. Without loss of generality, it is assumed that $\Omega = \Omega_1 \cup \Omega_2$, where Ω_1 and Ω_2 represent the subdomains for the PEC and the dielectric bodies, respectively. An electromagnetic field $\{\mathbf{E}^{\text{inc}}, \mathbf{H}^{\text{inc}}\}$, which originates in free space represented by subdomain Ω_0, is incident on the composite scatter. The permittivity, permeability, and intrinsic impedance in Ω_0 and Ω_2 are $\{\varepsilon_0, \mu_0, \eta_0\}$ and $\{\varepsilon_2, \mu_2, \eta_2\}$, respectively.

Fig. 1 shows these three subdomains used by the MT-DD-SIE formulation: Ω_0, Ω_1, and Ω_2. The boundaries of these subdomain are $\partial\Omega_0$, $\partial\Omega_1$, and $\partial\Omega_2$, and $\hat{\mathbf{n}}_0$, $\hat{\mathbf{n}}_1$, and $\hat{\mathbf{n}}_2$ are the inward pointing unit normal vectors on these boundaries. Equivalent unknown (electric and normalized magnetic) currents $\{\mathbf{J}_0, \mathbf{M}_0\}$, $\mathbf{J}_1$, and $\{\mathbf{J}_2, \mathbf{M}_2\}$ are introduced on $\partial\Omega_0$, $\partial\Omega_1$, and $\partial\Omega_2$, respectively.

Let Γ_{ij}, $i, j \in \{0, 1, 2\}$ denote an interface between any two subdomains Ω_i and Ω_j. On Γ_{20} and Γ_{02}, i.e., the interfaces between the subdomains of free space and the dielectric body, RTCs described in [25] are used. On Γ_{01}, Γ_{10}, Γ_{21}, and Γ_{12}, i.e., the interfaces between the PEC subdomain and the other two subdomains, the following RTCs are enforced:

$$\eta_0\mathbf{J}_0 - \eta_0\hat{\mathbf{n}}_0 \times \mathbf{M}_0 + \eta_0\mathbf{J}_1 = 0, \text{ on } \Gamma_{01}$$
$$\eta_0\hat{\mathbf{n}}_0 \times \mathbf{J}_0 + \eta_0\mathbf{M}_0 - \eta_0\hat{\mathbf{n}}_1 \times \mathbf{J}_1 = 0, \text{ on } \Gamma_{01} \quad (1)$$
$$\eta_0\mathbf{J}_1 + \eta_0\mathbf{J}_0 + \eta_0\hat{\mathbf{n}}_0 \times \mathbf{M}_0 = 0, \text{ on } \Gamma_{10} \quad (2)$$
$$\eta_2\mathbf{J}_2 - \eta_0\hat{\mathbf{n}}_2 \times \mathbf{M}_2 + \eta_2\mathbf{J}_1 = 0, \text{ on } \Gamma_{21}$$
$$\eta_2\hat{\mathbf{n}}_2 \times \mathbf{J}_2 + \eta_0\mathbf{M}_2 - \eta_2\hat{\mathbf{n}}_1 \times \mathbf{J}_1 = 0, \text{ on } \Gamma_{21} \quad (3)$$
$$\eta_0\mathbf{J}_1 + \eta_0\mathbf{J}_2 + \eta_0\hat{\mathbf{n}}_2 \times \mathbf{M}_2 = 0, \text{ on } \Gamma_{12}. \quad (4)$$

Note that a simple algebraic manipulation on (1)–(2) and (3)–(4) shows that they are equivalent to the PEC boundary conditions $\hat{\mathbf{n}}_0 \times \mathbf{M}_0 = 0$, on Γ_{01} and $\hat{\mathbf{n}}_2 \times \mathbf{M}_2 = 0$, on $\in \Gamma_{21}$, respectively. In Ω_1, (2) and (4) are used as the governing equations. For Ω_0 and Ω_2, RTCs on Γ_{01}, Γ_{02}, and Γ_{20}, Γ_{21} are, respectively, combined with EFIE and MFIE to yield the governing equations as

$$\frac{\eta_0}{2}\mathbf{J}_0 + \eta_0\hat{\mathbf{n}}_0 \times \hat{\mathbf{n}}_0 \times \left\{\mathcal{L}_0[\mathbf{J}_0] - \overline{\mathcal{K}}_0[\mathbf{M}_0]\right\}$$
$$+ \frac{\eta_0}{2}\mathbf{J}_1 = -\hat{\mathbf{n}}_0 \times \hat{\mathbf{n}}_0 \times \mathbf{E}^{\text{inc}}, \text{on } \Gamma_{01}$$
$$\frac{\eta_0}{2}\mathbf{M}_0 + \eta_0\hat{\mathbf{n}}_0 \times \hat{\mathbf{n}}_0 \times \left\{\mathcal{L}_0[\mathbf{M}_0] + \overline{\mathcal{K}}_0[\mathbf{J}_0]\right\}$$
$$- \frac{\eta_0}{2}\hat{\mathbf{n}}_1 \times \mathbf{J}_1 = -\eta_0\hat{\mathbf{n}}_0 \times \hat{\mathbf{n}}_0 \times \mathbf{H}^{\text{inc}}, \text{on } \Gamma_{01} \quad (5)$$

$$\frac{\eta_0}{2}\mathbf{J}_0 + \eta_0\hat{\mathbf{n}}_0 \times \hat{\mathbf{n}}_0 \times \left\{\mathcal{L}_0[\mathbf{J}_0] - \overline{\mathcal{K}}_0[\mathbf{M}_0]\right\}$$
$$+ \frac{\eta_0}{2}\left\{\mathbf{J}_2 + \hat{\mathbf{n}}_2 \times \mathbf{M}_2\right\} = -\hat{\mathbf{n}}_0 \times \hat{\mathbf{n}}_0 \times \mathbf{E}^{\text{inc}}, \text{on } \Gamma_{02}$$
$$\frac{\eta_0}{2}\mathbf{M}_0 + \eta_0\hat{\mathbf{n}}_0 \times \hat{\mathbf{n}}_0 \times \left\{\mathcal{L}_0[\mathbf{M}_0] + \overline{\mathcal{K}}_0[\mathbf{J}_0]\right\}$$
$$+ \frac{\eta_0}{2}\left\{\mathbf{M}_2 - \hat{\mathbf{n}}_2 \times \mathbf{J}_2\right\} = -\eta_0\hat{\mathbf{n}}_0 \times \hat{\mathbf{n}}_0 \times \mathbf{H}^{\text{inc}}, \text{on } \Gamma_{02} \quad (6)$$

$$\frac{\eta_2}{2}\mathbf{J}_2 + \hat{\mathbf{n}}_2 \times \hat{\mathbf{n}}_2 \times \left\{\eta_2\mathcal{L}_2[\mathbf{J}_2] - \eta_0\overline{\mathcal{K}}_2[\mathbf{M}_2]\right\}$$
$$+ \frac{1}{2}\left\{\eta_2\mathbf{J}_0 + \eta_0\hat{\mathbf{n}}_0 \times \mathbf{M}_0\right\} = 0, \text{ on } \Gamma_{20}$$
$$\frac{\eta_0}{2}\mathbf{M}_2 + \hat{\mathbf{n}}_2 \times \hat{\mathbf{n}}_2 \times \left\{\eta_0\mathcal{L}_2[\mathbf{M}_2] + \eta_2\overline{\mathcal{K}}_2[\mathbf{J}_2]\right\}$$
$$+ \frac{1}{2}\left\{\eta_0\mathbf{M}_0 - \eta_2\hat{\mathbf{n}}_0 \times \mathbf{J}_0\right\} = 0, \text{ on } \Gamma_{20} \quad (7)$$
$$\frac{\eta_2}{2}\mathbf{J}_2 + \hat{\mathbf{n}}_2 \times \hat{\mathbf{n}}_2 \times \left\{\eta_2\mathcal{L}_2[\mathbf{J}_2] - \eta_0\overline{\mathcal{K}}_2[\mathbf{M}_2]\right\}$$
$$+ \frac{\eta_2}{2}\mathbf{J}_1 = 0, \text{on } \Gamma_{21}$$
$$\frac{\eta_0}{2}\mathbf{M}_2 + \hat{\mathbf{n}}_2 \times \hat{\mathbf{n}}_2 \times \left\{\eta_0\mathcal{L}_2[\mathbf{M}_2] + \eta_2\overline{\mathcal{K}}_2[\mathbf{J}_2]\right\}$$
$$- \frac{1}{2}\left\{\eta_2\hat{\mathbf{n}}_1 \times \mathbf{J}_1\right\} = 0, \text{ on } \Gamma_{21}. \quad (8)$$

In (5)–(8), $\mathcal{L}_j[.]$ and $\overline{\mathcal{K}}_j[.]$ are the well-known SIE operators associated with the Stratton–Chu representation of the electromagnetic fields in Ω_j (see, for example, [25]). Equations (2), (4), and (5)–(8) form a coupled set in unknowns $\{\mathbf{J}_0, \mathbf{M}_0\}$, $\mathbf{J}_1$, and $\{\mathbf{J}_2, \mathbf{M}_2\}$. The solution of this system is carried out numerically, as described in the next section.

Several observations about (2), (4), and (5)–(8) are in order: First, the coupling between a given subdomain and its neighbors is facilitated using RTCs defined at the interfaces between them. This coupling is local and results in sparse (off-diagonal) matrix blocks. Second, no EFIE or MFIE-type SIEs are required on $\partial\Omega_1$ (the surface of the PEC body), the only governing equations are PEC-RTCs (2) and (4). Their discretization results in a sparse (diagonal) matrix block.

B. Numerical Solution

To facilitate the numerical solution of the coupled system of (2), (4), and (5)–(8), $\{\mathbf{J}_0, \mathbf{M}_0\}$, $\mathbf{J}_1$, and $\{\mathbf{J}_2, \mathbf{M}_2\}$ are expanded using the RWG basis functions [26]. Inserting this expansion into the coupled system and applying Galerkin testing yield a linear system of equations

$$\begin{bmatrix} \mathbf{A}_0 & \mathbf{M}_{01}^{\mathrm{ij}} & \mathbf{M}_{02}^{\mathrm{ii}} \\ \mathbf{M}_{10}^{\mathrm{ji}} & \mathbf{G}_1 & \mathbf{M}_{12}^{\mathrm{ji}} \\ \mathbf{M}_{20}^{\mathrm{ii}} & \mathbf{M}_{21}^{\mathrm{ij}} & \mathbf{A}_2 \end{bmatrix} \begin{bmatrix} \mathbf{I}_0 \\ \mathbf{I}_1 \\ \mathbf{I}_2 \end{bmatrix} = \begin{bmatrix} \mathbf{V}_0 \\ \mathbf{0} \\ \mathbf{0} \end{bmatrix}. \tag{9}$$

Here, $\mathbf{I}_0$, $\mathbf{I}_1$, and $\mathbf{I}_2$ are the vectors storing the unknown coefficients of the RWG expansions of $\{\mathbf{J}_0, \mathbf{M}_0\}$, $\mathbf{J}_1$, and $\{\mathbf{J}_2, \mathbf{M}_2\}$, respectively. $\mathbf{V}_0 = [\mathbf{V}_0^{\mathrm{j}}, \mathbf{V}_0^{\mathrm{m}}]$ is the vector of tested incident fields that are expressed as

$$\begin{aligned} \mathbf{V}_0^{\mathrm{j}} &= -\left\langle \mathbf{j}_0, \hat{\mathbf{n}}_0 \times \hat{\mathbf{n}}_0 \times \mathbf{E}^{\mathrm{inc}} \right\rangle_{\partial\Omega_0} \\ \mathbf{V}_0^{\mathrm{m}} &= -\eta_0 \left\langle \mathbf{m}_0, \hat{\mathbf{n}}_0 \times \hat{\mathbf{n}}_0 \times \mathbf{H}^{\mathrm{inc}} \right\rangle_{\partial\Omega_0} \end{aligned} \tag{10}$$

where $\langle ., . \rangle$ is the inner product between, and $\mathbf{j}_m$ and $\mathbf{m}_m$ represent the sets of RWG functions used to expand $\mathbf{J}_m$ and $\mathbf{M}_m$, respectively. In (9), $\mathbf{A}_0$ and $\mathbf{A}_2$ are dense matrix blocks corresponding to the self-interactions in Ω_0 and Ω_2, respectively, and their expressions can be found in [25]. Note that $\mathbf{A}_0$ and $\mathbf{A}_2$ are well-conditioned and diagonally dominant just like the matrices arising from the discretization of CFIE. Similarly, $\mathbf{G}_1$ is the matrix block that corresponds to the self-interactions on Ω_1 and it is expressed as

$$\mathbf{G}_1 = \frac{\eta_0}{2} \langle \mathbf{j}_1, \mathbf{j}_1 \rangle_{\partial\Omega_1}. \tag{11}$$

$\mathbf{G}_1$ is sparse and well-conditioned. This is due to the use of PEC-RTCs (2) and (4) as governing equations on Ω_1. In (10), $\mathbf{M}_{mn}$ are the matrix blocks that correspond to the coupling between Ω_m and Ω_n, and they are expressed as

$$\mathbf{M}_{mn}^{\mathrm{ii}} = \begin{bmatrix} \frac{\eta_m}{2} \langle \mathbf{j}_m, \mathbf{j}_n \rangle_{\Gamma_{mn}} & \frac{\eta_0}{2} \langle \mathbf{j}_m, \hat{\mathbf{n}}_n \times \mathbf{m}_n \rangle_{\Gamma_{mn}} \\ \frac{\eta_0}{2} \langle \mathbf{m}_m, \hat{\mathbf{n}}_n \times \mathbf{j}_n \rangle_{\Gamma_{mn}} & -\frac{\eta_m}{2} \langle \mathbf{m}_m, \mathbf{m}_n \rangle_{\Gamma_{mn}} \end{bmatrix} \tag{12}$$

$$\mathbf{M}_{mn}^{\mathrm{ij}} = \begin{bmatrix} \frac{\eta_m}{2} \langle \mathbf{j}_m, \mathbf{j}_n \rangle_{\Gamma_{mn}} \\ \frac{\eta_0}{2} \langle \mathbf{m}_m, \hat{\mathbf{n}}_n \times \mathbf{j}_n \rangle_{\Gamma_{mn}} \end{bmatrix} \tag{13}$$

$$\mathbf{M}_{mn}^{\mathrm{ji}} = \begin{bmatrix} \frac{\eta_m}{2} \langle \mathbf{j}_m, \mathbf{j}_n \rangle_{\Gamma_{mn}} & \frac{\eta_0}{2} \langle \mathbf{j}_m, \hat{\mathbf{n}}_n \times \mathbf{m}_n \rangle_{\Gamma_{mn}} \end{bmatrix}. \tag{14}$$

$\mathbf{M}_{mn}$ are sparse. This is due to use of RTCs to account for coupling between any two subdomains.

Several comments about the matrix system in (9) are as follows.

1) Since $\mathbf{G}_1$ is well-conditioned, it does not negatively affect the convergence of the iterative scheme used to solve (9).
2) Indeed, FGMRES, an inner–outer iteration scheme described in [25] and [27], is used here. Note that FGMRES uses a lower triangular right preconditioner constructed using the blocks of the matrix in (9), as explained in detail in [25].
3) This iterative scheme as applied to the solution of (9) is significantly faster than CRM [11], which makes use of EFIE-PMCHWT to account for PEC/dielectric composite objects. Additionally, since the coupling matrices in (9) are sparse, the resulting solver has a smaller memory footprint. These benefits are demonstrated by the numerical results presented in Section III. Note that even though the formulation and the discretization scheme described here are developed for a problem with three subdomains (for the sake of simplicity in the description), MT-DD-SIE allows for an arbitrary number of PEC/dielectric subdomains.

III. Numerical Results

In this section, the accuracy, the efficiency, and the applicability of the extended MT-DD-SIE are demonstrated via numerical examples. In all examples, the scatterers are nonmagnetic and the excitation is a planewave with frequency f and electric field $\mathbf{E}^{\mathrm{inc}}(\mathbf{r}) = E_0 \hat{\mathbf{p}} e^{-j\hat{\mathbf{k}}\cdot\mathbf{r}}$, where $E_0 = 1\,\mathrm{V/m}$ is the amplitude, $\hat{\mathbf{p}}$ is the polarization vector, and $\hat{\mathbf{k}}$ is the direction of propagation. The accuracy and the efficiency of MT-DD-SIE is compared to those of CRM and the method proposed in [24]. The method in [24] is referred to as MT-PMCHWT in the rest of this section. MT-DD-SIE and MT-PMCHWT use the same geometry discretization. The average edge length in this discretization and the one used by CRM is 0.1λ (unless otherwise stated), where λ is the wavelength in free space at f. The FGMRES iterations for MT-DD-SIE and the GMRES iterations for CRM and MT-PMCHWT are terminated when the relative residual reaches 0.001. Note that CRM does not use any preconditioner since its memory requirement is already much larger than that of MT-DD-SIE. MT-DD-SIE uses the preconditioner described in [25] and MT-PMCHWT is tested for two cases, without a preconditioner and with a sparse approximate inverse (SAI) preconditioner.

A. Dielectric-Coated PEC Sphere

In the first example, electromagnetic scattering from a dielectric-coated PEC sphere is analyzed. The radius of the sphere is $0.5\,\mathrm{m}$, the thickness of the coating is $0.1\,\mathrm{m}$, and its relative permittivity is 2.0. Planewave parameters $f = 0.3\,\mathrm{GHz}$, $\hat{\mathbf{p}} = \hat{\mathbf{x}}$, and $\hat{\mathbf{k}} = \hat{\mathbf{z}}$. MT-DD-SIE decomposes the scatterer into three subdomains: free space, dielectric coating, and PEC sphere. To demonstrate the accuracy of MT-DD-SIE and CRM, the relative root-mean-square error (RMSE) in radar cross section (RCS), which is defined as

$$\mathrm{RMSE} = \sqrt{\frac{\sum_{i=0}^{N} \left| \sigma(i\Delta\theta, \phi) - \sigma^{\mathrm{ref}}(i\Delta\theta, \phi) \right|^2}{\sum_{i=0}^{N} \left| \sigma^{\mathrm{ref}}(i\Delta\theta, \phi) \right|^2}} \tag{15}$$

is computed for different levels of discretization. Here, σ is the RCS computed using MT-DD-SIE or CRM, σ^{ref} is the reference RCS computed using the Mie series, $N = 180$, $\Delta\theta = 1.0^\circ$, and

TABLE I
RMSE IN RCS OF THE COATED SPHERE

Element size	0.1λ	0.05λ	0.025λ
MT-DD-SIE	0.0301	0.0069	0.0014
CRM	0.0306	0.0071	0.0018

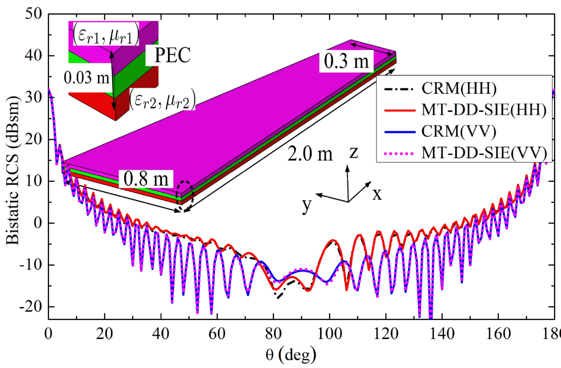

Fig. 2. Bistatic RCS of the three-layer composite plate.

TABLE II
COMPUTATIONAL REQUIREMENTS FOR THE THREE-LAYER PLATE

	Time	Memory	Iterations
MT-DD-SIE	30 m	4.74 GB	141
CRM	3 h 55 m	12.5 GB	4 148

$\phi = 0$. As shown in Table I, both methods achieve the same accuracy for the same level of discretization.

B. Three-Layer Plate

In this example, electromagnetic scattering from a three-layer plate is analyzed (see Fig. 2). The relative permittivities of the dielectric layers (located on top and bottom of the PEC layer) are 3.0 and 2.0, respectively. Two sets of simulations are carried out with planewave parameters $f = 3.0$ GHz, $\hat{\mathbf{p}} \in \{\hat{\mathbf{x}}, \hat{\mathbf{y}}\}$, and $\hat{\mathbf{k}} = -\hat{\mathbf{z}}$. MT-DD-SIE decomposes the scatterer into four subdomains with unknown numbers of 155 010, 141 746, 71 136, and 142 272. The number of unknowns for CRM is 355 154.

The RCS computed by MT-DD-SIE and CRM on the xz plane for two different polarizations are shown in Fig. 2. The results agree very well. The computation time and the memory required by the two methods are shown in Table II. Both methods are executed on a personal computer with Intel Core i7-7700 K @ 4.20 GHz CPU. The table clearly shows the benefits of MT-DD-SIE over CRM.

C. Dielectric-Coated PEC UAV

In the last example, electromagnetic scattering from a dielectric-coated PEC UAV is analyzed (see Fig. 3). The relative permittivity of the coating is $2.0 - 1.0j$. Planewave parameters $f = 1.0$ GHz, $\hat{\mathbf{p}} = \hat{\mathbf{x}}$, and $\hat{\mathbf{k}} = -\hat{\mathbf{z}}$. MT-DD-SIE decomposes the scatterer into three subdomains: free space, dielectric coating, and PEC UAV surface with number of unknowns of 182 052, 364 104, and 182 052, respectively. The total numbers of unknowns for MT-DD-SIE and MT-PMCHWT and CRM are 1 274 364 and 910 260, respectively. Figs. 3 and 4 present the electric currents induced on the surface of the UAV's coating and the RCS of the whole scatterer on the xz plane as computed

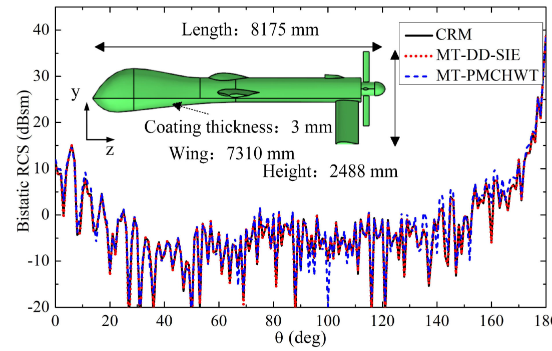

Fig. 3. Geometry of the dielectric-coated PEC UAV (inset) and its RCS.

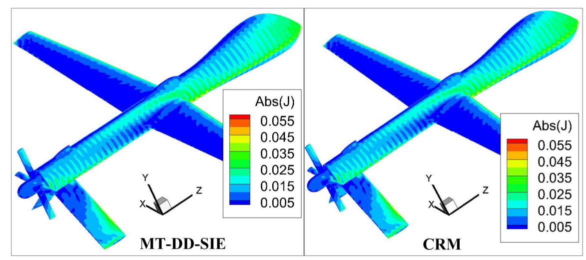

Fig. 4. Electric currents induced on the surface of the UAV's coating.

TABLE III
COMPUTATIONAL REQUIREMENTS FOR THE COATED UAV

	Time	Memory	Iterations
MT-DD-SIE	1 h 29 m	14.12 GB	82
CRM	45 h	28.22 GB	7 517
MT-PMCHWT (no pre.)	5 h 35 m	12.31 GB	1 010
MT-PMCHWT (SAI pre.)	4 h 8 m	18.41 GB	110

by MT-DD-SIE, CRM, and MT-PMCHWT, respectively. Fig. 3 shows that the results produced by the three methods agree well. The computation time and the memory required by these methods are shown in Table III. All methods are executed on a workstation with two 64 b Intel Xeon Gold 6148 at 2.40 GHz CPUs and 20 openMP parallel threads are utilized. MT-DD-SIE is 30 times faster than CRM and requires only about half the memory. Also compared to MT-PMCHWT, MT-DD-SIE has clear advantages.

IV. CONCLUSION

The MT-DD-SIE formulation is extended to efficiently account for PEC subdomains. The PEC subdomains are coupled to the dielectric subdomains via the use of PEC-RTCs. These RTCs are the only governing equations used for the PEC subdomains, and upon discretization, they yield well-conditioned (sparse) matrix blocks. This helps to maintain the well-conditioning of the whole MT-DD-SIE matrix system, which consists of sparsely coupled matrix blocks representing governing equations of the (dielectric and PEC) subdomains.

Numerical results show that this extended MT-DD-SIE method has clear advantages over the traditional CRM that makes use of EFIE-PMCHWT: For the same accuracy level, it is significantly faster (due to the increased iterative convergence) and has a smaller memory footprint.

References

[1] Z. He, D. Z. Ding, and R. S. Chen, "An efficient marching-on-in-degree solver of surface integral equation for multilayer thin medium-coated conductors," *IEEE Antennas Wireless Propag. Lett.*, vol. 15, pp. 1458–1461, 2016.

[2] B. Kong and X. Sheng, "An efficient preconditioning approach for surface MLFMA solution of scattering from multilayer dielectric bodies," *IEEE Antennas Wireless Propag. Lett.*, vol. 16, pp. 1192–1195, 2017.

[3] Z. He, Z. H. Fan, D. Z. Ding, and R. S. Chen, "Solution of PMCHW integral equation for transient electromagnetic scattering from dielectric body of revolution," *IEEE Trans. Antennas Propag.*, vol. 63, no. 11, pp. 5124–5129, Nov. 2015.

[4] W. J. Zhao, L. W. Li, and K. Xiao, "Analysis of electromagnetic scattering and radiation from finite microstrip structures using an EFIE-PMCHWT formulation," *IEEE Trans. Antennas Propag.*, vol. 58, no. 7, pp. 2468–2473, Jul. 2010.

[5] W. J. Zhao, L. W. Li, E. P. Li, and K. Xiao, "Analysis of radiation characteristics of conformal microstrip arrays using adaptive integral method," *IEEE Trans. Antennas Propag.*, vol. 60, no. 2, pp. 1176–1181, Feb. 2012.

[6] Ö. Ergül and L. Gürel, "Comparison of integral-equation formulations for the fast and accurate solution of scattering problems involving dielectric objects with the multilevel fast multipole algorithm," *IEEE Trans. Antennas Propag.*, vol. 57, no. 1, pp. 176–187, Jan. 2009.

[7] P. Ylä-Oijala and M. Taskinen, "Application of combined field integral equation for electromagnetic scattering by dielectric and composite objects," *IEEE Trans. Antennas Propag.*, vol. 53, no. 3, pp. 1168–1173, Mar. 2005.

[8] P. Ylä-Oijala and M. Taskinen, "Improving conditioning of electromagnetic surface integral equations using normalized field quantities," *IEEE Trans. Antennas Propag.*, vol. 55, no. 1, pp. 178–185, Jan. 2007.

[9] D. M. Solís, J. M. Taboada, O. Rubiños-López, and F. Obelleiro, "Improved combined tangential formulation for electromagnetic analysis of penetrable bodies," *J. Opt. Soc. Amer. B*, vol. 32, no. 9, pp. 1780–1787, Sep. 2015.

[10] P. Ylä-Oijala, P. Taskinen, and J. Sarvas, "Surface integral equation method for general composite metallic and dielectric structures with junctions," *Prog. Electromagn. Res.*, vol. 52, pp. 81–108, 2005.

[11] Y. Chu, W. C. Chew, J. Zhao, and S. Y. Chen, "A surface integral equation formulation for low-frequency scattering from a composite object," *IEEE Trans. Antennas Propag.*, vol. 51, no. 10, pp. 2837–2844, Oct. 2003.

[12] D. M. Solís, V. F. Martín, M. G. Araújo, D. Larios, F. Obelleiro, and J. M. Taboada, "Accurate EMC engineering on realistic platforms using an integral equation domain decomposition approach," *IEEE Trans. Antennas Propag.*, vol. 68, no. 4, pp. 3002–3015, Apr. 2020.

[13] V. F. Martín, D. Larios, D. M. Solís, J. M. Taboada, L. Landesa, and F. Obelleiro, "Tear-and-interconnect domain decomposition scheme for solving multiscale composite penetrable objects," *IEEE Access*, vol. 8, pp. 107345–107352, 2020.

[14] Z. Peng, K. H. Lim, and J. F. Lee, "Computations of electromagnetic wave scattering from penetrable composite targets using a surface integral equation method with multiple traces," *IEEE Trans. Antennas Propag.*, vol. 61, no. 1, pp. 256–270, Jan. 2013.

[15] J. Hu *et al.*, "Domain decomposition method based on integral equation for solution of scattering from very thin, conducting cavity," *IEEE Trans. Antennas Propag.*, vol. 62, no. 10, pp. 5344–5348, Oct. 2014.

[16] R. Zhao, J. Hu, H. P. Zhao, M. Jiang, and Z. P. Nie, "EFIE-PMCHWT based domain decomposition method for solving electromagnetic scattering from complex dielectric/metallic composite objects," *IEEE Antennas Wireless Propag. Lett*., vol. 16, pp. 1293–1296, 2017.

[17] J. Guan, S. Yan, and J. M. Jin, "A multisolver scheme based on Robin transmission conditions for electromagnetic modeling of highly complex objects," *IEEE Trans. Antennas Propag.*, vol. 64, no. 12, pp. 5345–5358, Dec. 2016.

[18] J. Guan, S. Yan, and J.-M. Jin, "A multi-solver scheme based on combined field integral equations for electromagnetic modeling of highly complex objects," *IEEE Trans. Antennas Propag.*, vol. 65, no. 3, pp. 1236–1247, Mar. 2017.

[19] I. Sekulic, E. Ubeda, and J. M. Rius, "Versatile and accurate schemes of discretization for the electromagnetic scattering analysis of arbitrarily shaped piecewise homogeneous objects," *J. Comput. Phys*., vol. 374, pp. 478–494, 2018.

[20] Z. Peng, "A novel multitrace boundary integral equation formulation for electromagnetic cavity scattering problems," *IEEE Trans. Antennas Propag.*, vol. 63, no. 10, pp. 4446–4457, Oct. 2015.

[21] R. Hiptmair and C. Jerez-Hanckes, "Multiple traces boundary integral formulation for Helmholtz transmission problems," *Adv. Comput. Math.*, vol. 37, no. 1, pp. 39–91, Jul. 2012.

[22] R. Hiptmair, C. Jerez-Hanckes, J. F. Lee, and Z. Peng, "Domain decomposition for boundary integral equations via local multi-trace formulations," in *Domain Decomposition Methods in Science and Engineering XXI*, vol. 98. New York, NY, USA: Springer, 2014, pp. 43–57.

[23] L. Zhang, S. F. Tao, Z. H. Fan, and R. S. Chen, "Mixed inner-outer iteration technique-based surface integral equations for fast solving EM scattering from penetrable objects," *IEEE Trans. Antennas Propag.*, vol. 66, no. 9, 4752–4758, Sep. 2018.

[24] R. Zhao, Z. X. Huang, W. F. Huang, J. Hu, and X. L. Wu, "Multiple-traces surface integral equations for electromagnetic scattering from complex microstrip structures," *IEEE Trans. Antennas Propag.*, vol. 66, no. 7, pp. 3804–3809, Jul. 2018.

[25] R. Zhao, Y. P. Chen, X. M. Gu, Z. X. Huang, H. Bagci, and J. Hu, "A local coupling multi-trace domain decomposition method for electromagnetic scattering from multilayered dielectric objects," *IEEE Trans. Antennas Propag.*, vol. 68, no. 10, pp. 7099–7108, Oct. 2020.

[26] S. M. Rao, D. R. Wilton, and A. W. Glisson, "Electromagnetic scattering by surfaces of arbitrary shape," *IEEE Trans. Antennas Propag.*, vol. AP-30, no. 3, pp. 409–418, May 1982.

[27] Y. Saad, "A flexible inner-outer preconditioned GMRES algorithm," *SIAM J. Sci. Comput.*, vol. 14, no. 2, pp. 461–469, 1993.

[28] Ö. Ergül and L. Gürel, "Fast and accurate analysis of large-scale composite structures with the parallel multilevel fast multipole algorithm," *J. Opt. Soc. Amer. A*, vol. 30, no. 3, pp. 509–517, Jan. 2013.

[29] A. Zhu and S. D. Gedney, "Comparison of the Müller and PMCHWT surface integral formulations for the locally corrected Nyström method," in *Proc. IEEE Antennas Propag. Soc. Symp.*, Monterey, CA, USA, Jun. 2004, pp. 3871–3874.

[30] P. Ylä-Oijala,, M. Taskinen, and S. Järvenpää, "Surface integral equation formulations for solving electromagnetic scattering problems with iterative methods," *Radio Sci.*, vol. 40, pp. 1–19, 2005.

[31] K. Cools, F. P. Andriulli, D. De Zutter, and E. Michielssen, "Accurate and conforming mixed discretization of the MFIE," *IEEE Antennas Wireless Propag. Lett.*, vol. 10, pp. 528–531, 2011.

[32] P. Ylä-Oijala, S. P. Kiminki, K. Cools, F. P. Andriulli, and S. Järvenpää, "Mixed discretization schemes for electromagnetic surface integral equations," *Int. J. Numer. Model.*, vol. 25, pp. 525–540, 2012.

[33] I. Bogaert, K. Cools, F. P. Andriulli, and H. Bagci, "Low-frequency scaling of the standard and mixed magnetic field and Müller integral equations," *IEEE Trans. Antennas Propag.*, vol. 62, no. 2, pp. 822–831, Feb. 2014.